J. Zool., Lond. (2004) **264**, 281–293 © 2004 The Zoological Society of London Printed in the United Kingdom DOI:10.1017/S0952836904005771

Respiratory turbinates of canids and felids: a quantitative comparison

Blaire Van Valkenburgh[1]*, Jessica Theodor[2], Anthony Friscia[1], Ari Pollack[1] and Timothy Rowe[3]

[1] Department of Ecology and Evolutionary Biology, University of California, Los Angeles, CA 90095-1606, U.S.A.
[2] Department of Geology, Illinois State Museum, 1011 East Ash Street, Springfield, IL 62703, U.S.A.
[3] Department of Geological Sciences, University of Texas, Austin, TX 78712, U.S.A.

(Accepted 31 March 2004)

Abstract

The respiratory turbinates of mammals are complex bony plates within the nasal chamber that are covered with moist epithelium and provide an extensive surface area for the exchange of heat and water. Given their functional importance, maxilloturbinate size and structure are expected to vary predictably among species adapted to different environments. Here the first quantitative analysis is provided of maxilloturbinate structure based on high-resolution computed tomography (CT) scans of the skulls of eight canid and seven felid species. The key parameters examined were the density of the maxilloturbinate bones within the nasal chamber and how that density varied along the air pathway. In both canids and felids, total maxilloturbinate chamber volume and bone volume increased with body size, with canids having *c*. 1.5–2.0 times the volume of maxilloturbinate than felids of similar size. In all species, the volume of the maxilloturbinates varies from rostral to caudal, with the peak volume occurring approximately midway, close to where airway cross-sectional area is greatest. Interspecific differences among canids or felids in maxilloturbinate density were not consistent with adaptive explanations, i.e. the densest maxilloturbinates were not associated with species living in arid or cold habitats. Some of the observed variation in maxilloturbinate form might reflect a need for both low- and high-resistance pathways for airflow under alternative conditions.

Key words: carnivorans, turbinates, respiration, nasal anatomy

INTRODUCTION

A key diagnostic feature of the class Mammalia is the presence of complex, bony scrolls within the nasal chamber known as the maxilloturbinates. Maxilloturbinates are one of three separate paired turbinates in the skull, each of which originates on a different bone: ethmoturbinates arise from the ethmoid, nasoturbinates from the nasal, and maxilloturbinates from the maxilla (Fig. 1). Ethmoturbinates are primarily if not entirely covered with olfactory epithelium and therefore involved in the sense of smell, whereas the maxilloturbinates and perhaps the nasoturbinates are covered with respiratory epithelium and function in modifying inspired air (Negus, 1958). The maxilloturbinates, also known as respiratory turbinates, are much larger and more complex than the nasoturbinates and lie directly along the pathway taken by air from nares to nasopharynx. Maxilloturbinates assist in both water and heat conservation and are well developed in mammals as a consequence of endothermy and associated increased ventilation rates (Schmidt-Nielsen, Hainsworth & Murrish, 1970; Hillenius, 1992). Inspired air is usually relatively cool and dry. As it passes over the moist, warm maxilloturbinates, air is warmed and fully saturated with water before reaching the lungs. On expiration, saturated air passes back across the just cooled maxilloturbinates and water condenses on to their surface. Empirical studies have shown that, on expiration, dogs can retain up to 75–80% of the heat and water that they add to each breath, simply by breathing through their nose (Goldberg, Langman & Taylor, 1981).

In addition to heat and water conservation, the maxilloturbinates probably play a role in what is known as 'selective brain cooling' (Baker, 1982). Selective brain cooling occurs when relatively cool venous blood from the maxilloturbinate surface returns to the heart via the cavernous sinus where it acts to cool arterial blood on its way to the brain. Laboratory experiments on artiodactyls, cats and dogs demonstrate that during exercise these species are capable of maintaining a differential between arterial blood temperature around the hypothalamus and that of the body (Hayward & Baker, 1969; Baker, 1982; Jessen, 2001). The rise in body temperature associated with exercise is not observed to the same degree at the hypothalamus. Initially it was argued that this protected the

*All correspondence to: B. Van Valkenburg.
E-mail: bvanval@ucla.edu

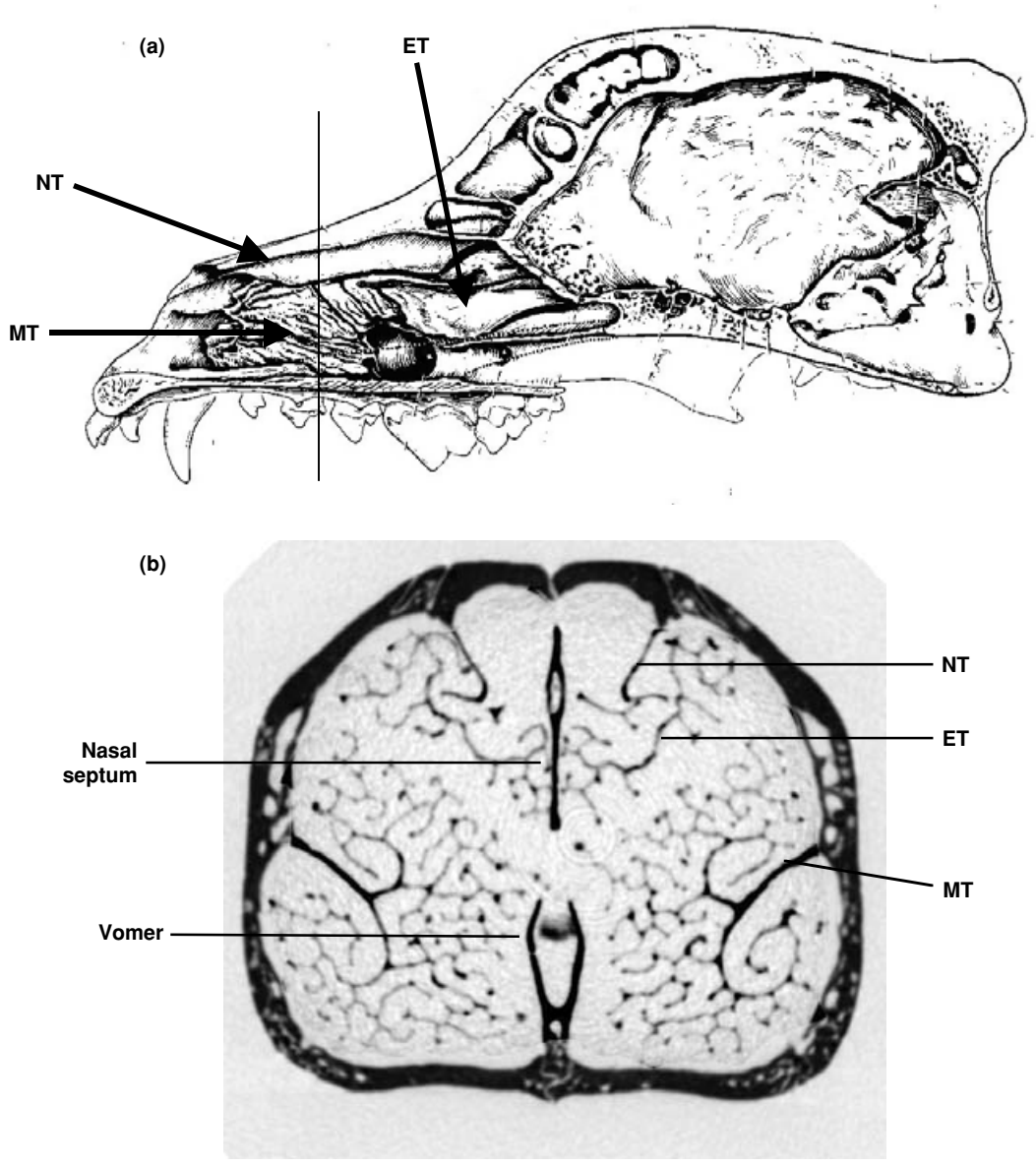

Fig. 1. (a) Domestic dog *Canis familiaris* skull sagittal section. (b) Inverted CT image of a coronal section of a kit fox *Vulpes macrotis* rostrum taken at approximately the position indicated by the vertical line on the dog skull. ET, ethmoturbinate; MT, maxilloturbinate; NT, nasoturbinate. (a) Modified from Evans (1993: fig. 4–47).

brain from the damaging effects of excess heat. However, recent experiments on free-ranging African artiodactyls indicate that brain temperature is often allowed to rise with body temperature during exercise (Mitchell, Maloney, Jessen *et al*., 2002 and references therein). Selective brain cooling is observed only during times of rest in the late afternoon when core body temperatures rise. At these times, cooling of the hypothalamus prevents the initiation of whole body cooling by evaporative water loss (sweating or panting). This conserves water and excess body heat can be radiated back to the environment at night by convection (Mitchell, Maloney, Jessen *et al*., 2002).

Given the functional importance of maxilloturbinates in heat and water conservation, it might be expected that their dimensions would vary in a predictable way among mammals of different size, habitats, or activity levels. Early studies of respiratory turbinate function focused on their apparently greater development in arid-adapted mammals such as camels, giraffes and kangaroo rats (Schmidt-Nielsen *et al*., 1970; Langman *et al*., 1979). Similarly, the complicated and extensive maxilloturbinates of pinnipeds probably reflects their relatively extreme needs for heat and water conservation (Negus, 1958; Huntley, Costa & Rubin, 1982; Mills & Christmas, 1990). Beyond these explorations of maxilloturbinate form in mammals adapted to extreme environments, there has been little investigation of possible correlations between respiratory turbinate form and environment. This may be because most of the variation in maxilloturbinate structure among mammals seems to be phylogenetic in origin (Negus, 1958). Ungulates tend to have rather simple open scrolls, for example, whereas carnivorans

tend to have more dendritic structures. Given the strong phylogenetic imprint, functional differences might be more apparent when comparing closely related species that share a common maxilloturbinate design. With this in mind, a study of species within two families of the order Carnivora, Canidae and Felidae was initiated, selecting species that differed in body mass and presumed water and heat conservation needs such as arctic (e.g. arctic fox *Alopex lagopus*), temperate (e.g. coyote *Canis latrans*) and tropical (e.g. Brazilian bush dog *Speothos venaticus*) species. High-speed runners (African wild dog *Lycaon pictus*, cheetah *Acinonyx jubatus*) were selected as well as less energetic species (e.g. grey fox *Urocyon cinereoargenteus*, lion *Panthera leo*).

The key parameters examined in this paper concern the density of the maxilloturbinate bones within the nasal chamber and how that density varies along the air pathway from rostral to caudal. Using mathematical models that assumed laminar flow, Collins, Pilkington & Schmidt-Nielsen (1971) and Schroter & Watkins (1989), argued that the distance between opposing maxilloturbinate surfaces (gap width) was critical to the efficient transfer of heat and water. Smaller gaps enhance the efficiency of transfer. Thus, it was expected that species from extremely cold and/or arid environments might show both denser packing and a greater volume of turbinate bones relative to body size. In addition, small species or those with relatively short snouts (e.g. felids) might be likely to have a denser packing of maxilloturbinate bones than large species because their short noses reduce the distance over which the exchange can occur. Moreover, given that the efficiency of transfer is also improved by increasing air transit time, it was predicted that in all species the maximum density of turbinate bone might occur where airflow slows. According to the principle of continuity, flow velocity in any pipe decreases when cross-sectional area increases (Vogel, 2003:37), and thus maxilloturbinate density should peak at or near the region of greatest cross-sectional area. Positioning peak maxilloturbinate density where airflow is slowest will also minimize the costs of pumping air across the turbinates and thus might be advantageous.

Joeckel *et al*. (2002) were the first to demonstrate that it was possible to resolve the delicate maxilloturbinate bones of carnivorans using computed tomography (CT) scans of dry skulls. In the past, studies of maxilloturbinate structure relied on sectioning skulls or entire heads, a destructive practice not favoured by many museums. With the advent of high-resolution CT, it now is possible to examine fine-scale internal structures non-destructively as is done here. Computed tomography scans have a number of advantages over anatomical sections. In addition to not destroying specimens, data are recorded permanently in digital format. Moreover, the data from each scan can be combined with those of other scans to produce a three-dimensional reconstruction of the skull that can be examined in all possible planes. At present, the only disadvantages of CT scans over anatomical sections are their expense and the challenges of analysing large quantities of data given a limited array of appropriate software. Thus, it is often necessary to create or modify software to answer a particular question.

Table 1. List of species and specimens scanned. FMNH, Field Museum of Natural History, Chicago; LACM, Natural History Museum of Los Angeles County; MVZ, Museum of Vertebrate Zoology, Berkeley, CA; UCLA, D. R. Dickey collection of the University of California, Los Angeles; BVV, personal collection of the senior author; C, Minnesota Department of Natural Resources, Forest Wildlife Population and Research Group. Sex: M, male; F, female; U, unknown

Species	Specimens	Sex
Canidae		
Arctic fox *Alopex lagopus*	UCLA 15161	M
	UCLA 15163	F
Kit fox *Vulpes macrotis*	UCLA HX 92	M
	UCLA HX 27	F
Red fox *V. vulpes*	UCLA 15267	M
Grey fox *Urocyon cinereoargenteus*	UCLA 6928	M
	UCLA E2	F
Coyote *Canis latrans*	UCLA 2739	M
	UCLA 1225	F
Grey wolf *C. lupus*	C476	M
	C460	F
African wild dog *Lycaon pictus*	BVV L1	U
	BVV L2	U
Bush dog *Speothos venaticus*	MVZ 184054	M
Felidae		
Lion *Panthera leo*	MVZ 117649	U
Leopard *P. pardus*	LACM 11704	M
Cheetah *Acinonyx jubatus*	FMNH 29635	M
	FMNH 127834	F
Puma *Puma concolor*	LACM 87430	M
	LACM 85440	F
Bobcat *Lynx rufus*	LACM 10115	M
	LACM 10118	F
African wild cat *Felis sylvestris lybica*	LACM 14480	M
	LACM 14474	F
Ocelot *Leopardus pardalis*	LACM 26789	F

METHODS

Eight canid and 7 felids were chosen for comparison, ranging in body mass from < 3 kg (kit fox *Vulpes macrotis*) to > 150 kg (African lion *Panthera leo*) (Table 1). Whenever possible, 2 adult skulls were scanned for each species, preferably male and female, of wild-caught individuals. Skulls were chosen for scanning if the maxilloturbinates seemed to be complete and undamaged when viewed from the external nares. Unfortunately, the fragile maxilloturbinates are frequently damaged post-mortem and this sometimes limited our sample. All skulls were scanned twice at the University of Texas (UT) High Resolution X-Ray Computed Tomography Facility. The initial scan was a low-resolution scan of the entire skull where coronal slice thickness ranged from 0.2 to 2 mm, depending on the size of the skull. A second higher resolution scan focused on the maxilloturbinate region at intervals ranging from 0.15 to 2 mm. It is recognized that a sample size of 1 or 2 individuals per species is not ideal,

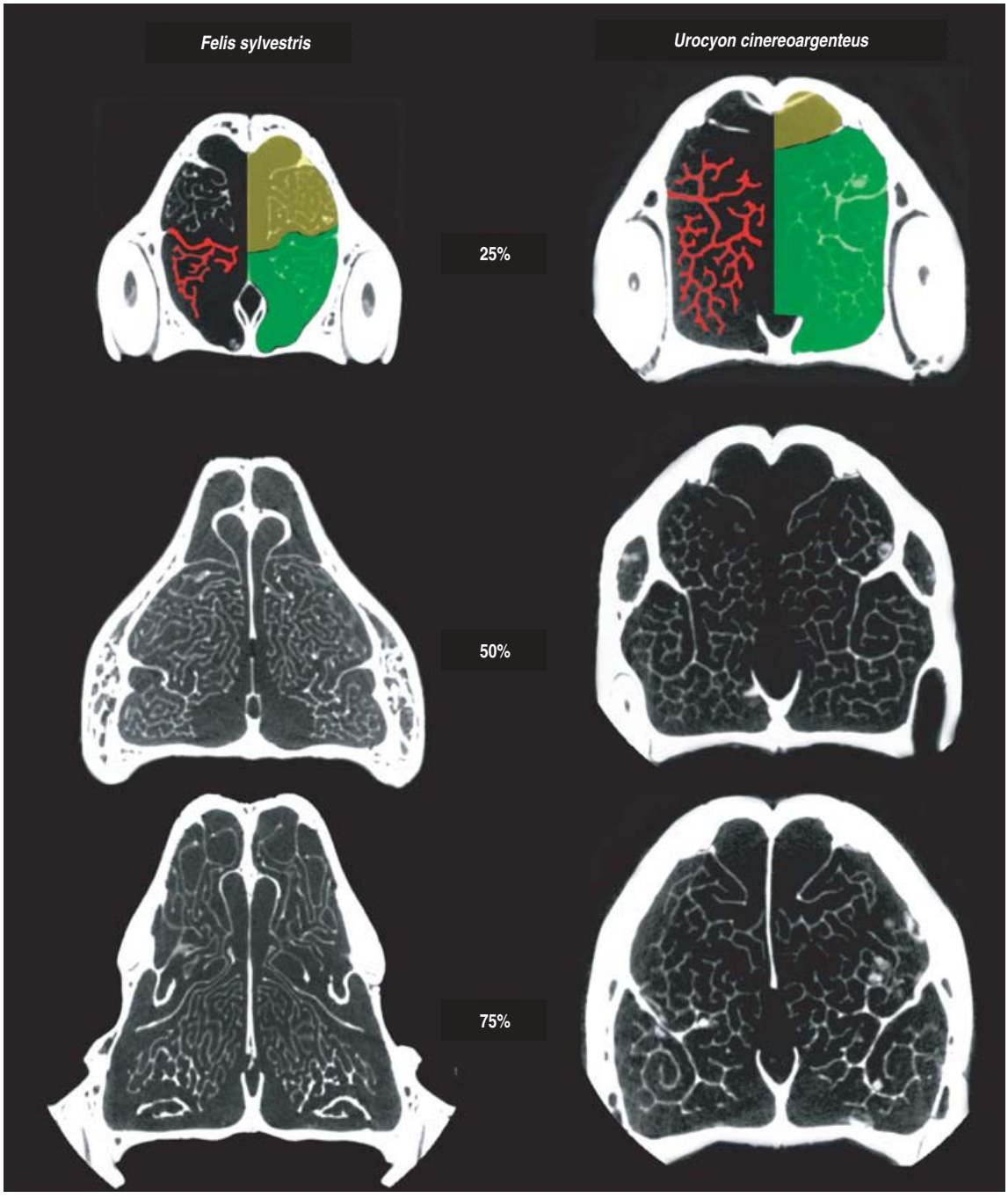

Fig. 2. Coronal slices (CT scans) of an African wild cat (left) and grey fox (right) skulls taken at three positions along length of maxilloturbinates: from anterior to posterior, at *c.* 25% (top), 50% (middle) and 75% (bottom), respectively. Maxilloturbinates on left side are highlighted in red, and region used to estimate maxilloturbinate chamber volume is highlighted in green on the opposite side in the two top scans. Nasal chamber volume included both the green and gold highlighted area.

but the costs of scanning are high and data collection from the many scans is labour intensive. All of the scans are available on the UT Digital Morphology Group website (http: //www.digimorph.org/).

The skull and maxilloturbinate scans produced *c*. 400 and 100 slices per skull, respectively. All scans were digitized using MNI Display, a program developed for the Montreal Neurological Institute for measuring human brain datasets. For each maxilloturbinate scan, threshold light intensity values were established for bone and air, and 2 regions were labelled for quantification, the portion of the nasal chamber that housed the maxilloturbinates (hereafter called the maxilloturbinate chamber or TC) as well as the entire nasal chamber (NC) (Fig. 2). Using the established threshold light intensity values, MNI Display measured the volume of maxilloturbinate bone (TV) for each scan in voxels (volumetric pixels). This provided us with the volume of maxilloturbinate bone per coronal

Table 2. Variable names, abbreviations, and definitions

Variable	Name	Definition
TV	Turbinate volume	Volume of maxilloturbinate bone in a single slice (CT scan)
TC	Turbinate chamber volume	Volume of the maxilloturbinate chamber in a single slice (CT scan)
NC	Nasal chamber volume	Volume of the nasal chamber in a single slice (CT scan)
TTV	Total turbinate volume	Sum of TV for all slices
TTC	Total turbinate chamber volume	Sum of TC for all slices
TNC	Total nasal chamber volume	Sum of NC for all slices

Table 3. Mean values of body mass (kg), estimated total turbinate volume (TTV), total turbinate chamber volume (TTC), and total nasal chamber volume (TNC) for all species. Body mass values were taken from the literature as noted

Species	Body mass	TTV (mm^3)	TTC (mm^3)	TNC (mm^3)
Arctic fox	3.5[a]	723.69	3893.38	4665.83
Kit fox	2.5[a]	289.21	1596.71	2402.13
Red fox	7[a]	793.12	3826	6718.24
Grey fox	4[a]	376.62	1864.36	3109.03
Coyote	13[a]	1980.91	12411.21	16269.63
Grey wolf	43[a]	8659.17	35663.09	43772.25
African wild dog	26[a]	5424.98	30791	36747.03
Bush dog	6[a]	1090.38	5569	7980.95
Lion	172[b]	22677.89	190608.5	516200
Leopard	45[b]	5924.59	34928.48	96683.23
Cheetah	58[b]	6256.34	25286.86	75584.22
Puma	68[b]	4871.68	25115.37	78660.02
Bobcat	10[b]	388.89	1849.99	9998.77
African wild cat	4.5[c]	141.18	940.17	3065.52
Ocelot	11.5[c]	306.35	2337.33	11075.54

[a] References cited in Van Valkenburgh & Koepfli, 1993.
[b] References cited in Van Valkenburgh, 1997.
[c] Sunquist & Sunquist, 2002.

slice, and by summing across all slices, an estimate of total maxilloturbinate volume (TTV). Our initial desire had been to measure maxilloturbinate surface area but this has proved to be more difficult owing to a lack of appropriate software. However, work is continuing towards this goal. If the plate-like maxilloturbinate bones are of similar thickness in all species regardless of body size, and if they are oriented perpendicular to the plane of the scan, as they seem to be, then the estimates of bone volume should be correlated with surface area. Although we could not be sure that all the maxilloturbinate plates were oriented exactly perpendicular to the scanning plane, the individual slice thickness (0.15–2 mm) was very fine relative to snout length and this should alleviate problems resulting from any bending of the plates relative to the scanning plane. Estimated nasal chamber volumes and turbinate chamber volumes, respectively, were summed for all slices to produce total chamber volumes (TTC, TNC).

Relationships among the measured variables (maxilloturbinate volume, chamber volumes) themselves, as well as between them and estimates of body size were explored with bivariate regressions in the program StatView. Variable names, their abbreviations and their definitions are given in Table 2. To explore the distribution of turbinate volume along the length of the maxilloturbinates, the total length of the turbinates was standardized for each skull to 100, and data extracted for 21 slices from front to back, in increments of 5% of the total distance. The results are presented for the middle 80% of turbinate length only because there seemed to be more variation in data collected from the extreme ends of the chamber. Rostrally, this reflected increased post-mortem damage to the delicate maxilloturbinates near the nasal opening. Caudally, the variation reflected poorer resolution of the maxilloturbinates as they diminished to very small size.

RESULTS

General description of canid and felid maxilloturbinates

Gross maxilloturbinate structure is often similar among mammals within the same order (Negus, 1958). For example, those of rodents exhibit a folded appearance, those of artiodactyls appear as a more open scroll, and those of carnivorans tend to have a branching architecture (Fig. 2). This is best expressed in our sample in the canids, all of which have an extensive arbour, both above and

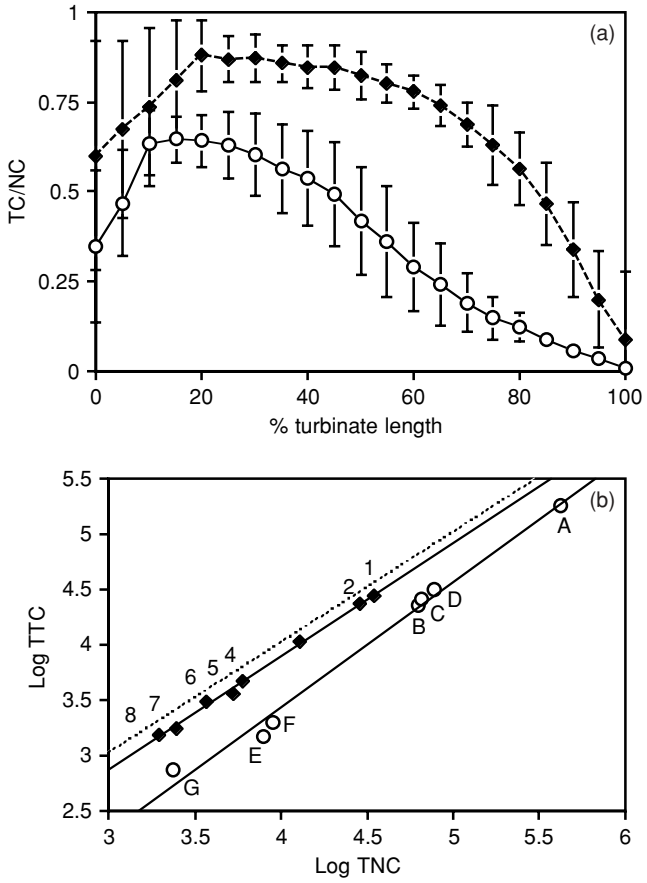

Fig. 3. (a) Average percentage of nasal chamber occupied by maxilloturbinate chamber in 21 coronal slices, taken at 5% intervals from rostral (0) to caudal (100) for canids (◆) and felids (○). Error bars are single standard deviations. (b) Linear regressions of $\log_{10}$ total turbinate chamber volume (TTC) plotted against $\log_{10}$ total nasal chamber volume (TNC) for canids and felids. For canids, $\log_{10}$ TTC = 1.03 ($\log_{10}$ TNC) − 0.224, $r^2 = 0.99$; for felids, $\log_{10}$ TTC = 1.13 ($\log_{10}$ TNC) − 1.16, $r^2 = 0.99$. Species: 1, grey wolf; 2, African wild dog; 3, coyote; 4, bush dog; 5, red fox; 6, arctic fox; 7, grey fox; 8, kit fox; A, African lion; B, cheetah; C, puma; D, leopard; E, bobcat; F, ocelot; G, African wild cat. Dashed line, equivalence of TTC and TNC.

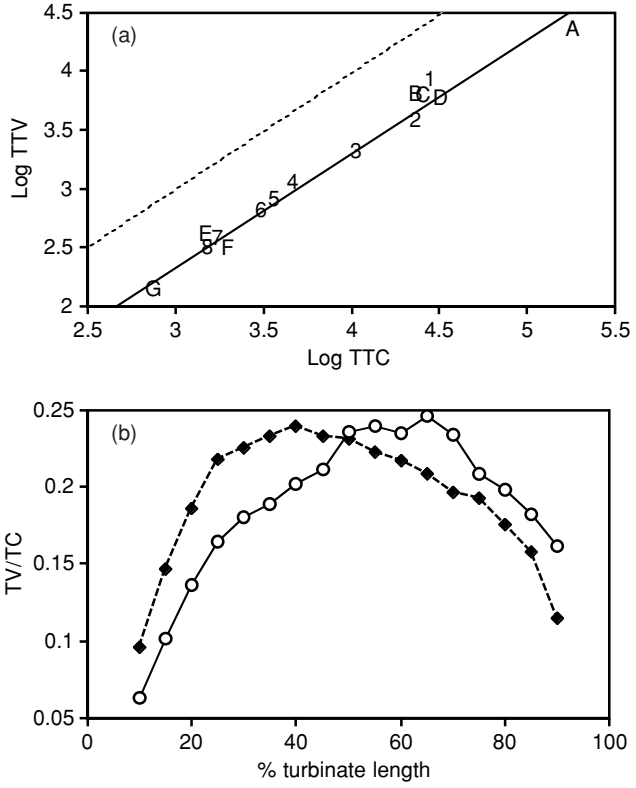

Fig. 4. (a) Linear regression of $\log_{10}$ total maxilloturbinate volume (TTV) plotted against $\log_{10}$ total maxilloturbinate chamber volume (TTC) for canids and felids; $\log_{10}$ TTV = 0.97 ($\log_{10}$ TTC) − 0.58, $r^2 = 0.98$. Species as in Fig. 3. Dashed line, equivalence of TTV and TTC. (b) Average percentage of maxilloturbinate chamber occupied by the maxilloturbinate bones (TV/TC) in each of 21 coronal slices, taken at 5% intervals from rostral (0) to caudal (100), for canids (◆) and felids (○).

below the bony root from the maxilla (Fig. 2). In both canids and felids, there is also a single scroll on each side that extends ventrally from the root. Often this scroll gives off multiple branches that vary in development among species. Unlike canids, felids have a very weak development of the maxilloturbinates dorsal to the bony stem (Fig. 2; Joeckel *et al*., 2002). Instead, this region of the nasal cavity is filled rostrally by fairly complex nasoturbinates and caudally by extensions of the ethmoturbinates. In canids, the nasoturbinates are simple, and the ethmoturbinates remain largely caudal and dorsal to the maxilloturbinates. Bivariate regression of the log of turbinate chamber volume against that of the nasal chamber reveals similar scaling (near isometry) in both felids and canids, but canids have a relatively larger turbinate chamber for a given snout size (Fig. 3). On average, the maxilloturbinates occupy 75–85% of nasal cavity volume in canids, whereas in felids they fill only 28–50% of the entire chamber (Table 3).

Maxilloturbinate density: canids *vs* felids

The total volume of maxilloturbinate bone (TTV) relative to the total volume of the maxilloturbinate chamber (TTC) is similar across our sample of canids and felids and nearly isometric (Fig. 4a). Thus, it seems that the packing of bone within the chamber is similar in small and large species when data from all slices are summed. However, this summation masks important rostral to caudal variation in maxilloturbinate packing that occurs within individuals as well as between species.

Maxilloturbinate packing for each coronal slice can be estimated by the ratio of the volume of the maxilloturbinates (TV) to that of the chamber (TC). In almost all species, the density of turbinate bone (TV/TC) increases caudally to a maximum and then declines. The position of maximum density differs in the two families (Fig. 4b).

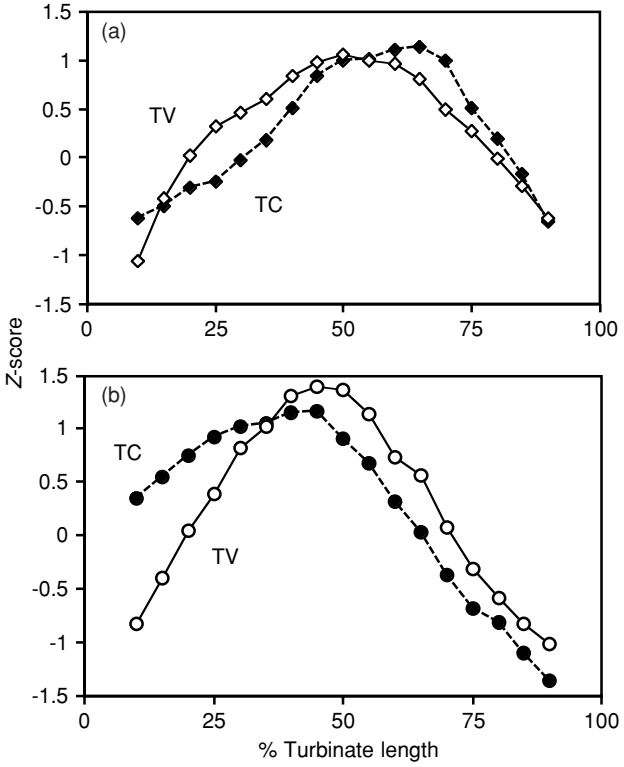

Fig. 5. Relationship between maximum turbinate volume and maximum chamber size. Maxilloturbinate volume (TV) and turbinate chamber volume (TC) expressed as *Z*- scores (standardized deviates of the mean) in 21 coronal slices, taken at 5% intervals from rostral (0) to caudal (100) for canids (a) and felids (b).

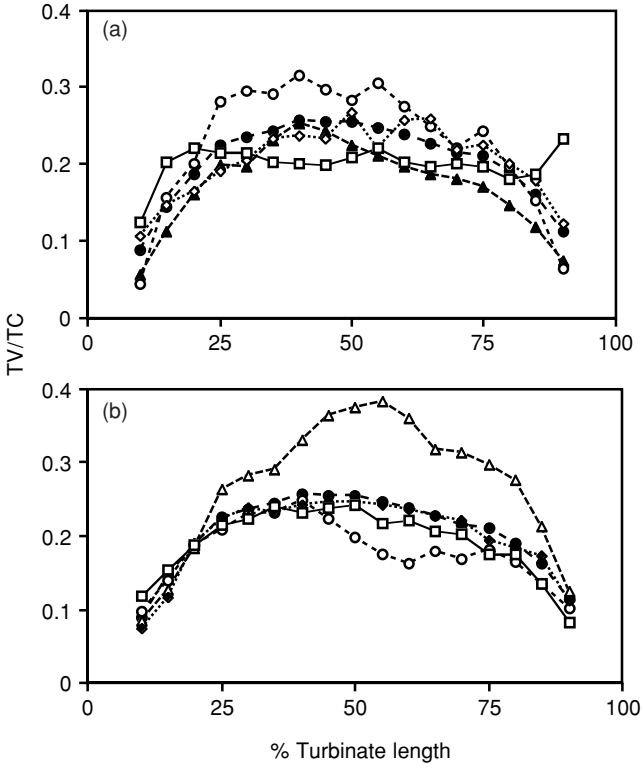

Fig. 6. Average percentage of maxilloturbinate chamber occupied by maxilloturbinate bones (TV/TC) in each of 21 coronal slices, taken at 5% intervals from rostral (0) to caudal (100), for each sampled canid. ●, Average of all eight species (both plots). (a) ○, bush dog; ◇, red fox; □, grey fox; ▲, coyote. (b) △, grey wolf; □, kit fox; ◆, arctic fox; ○, African wild dog.

In canids, the maximum is reached about midway, at 40% (range 30–55%) of the distance from the rostral to the caudal end of the maxilloturbinates. In felids, the maximum density tends to occur farther back, about 70% of total maxilloturbinate length, but ranges from 25% (leopard *Panthera pardus*) to 80% (lion). Maximum values of TV/TC for each species do not differ between canids and felids ($t = -1.29$, $P = 0.245$, d.f. $= 6$), even though felids have relatively shorter snouts and therefore less room to house maxilloturbinates.

The maximum volume of maxilloturbinates is expected to occur at or near the region of greatest cross-sectional area of the airway because it is here that airflow velocity will be minimal, favouring an efficient exchange of water and heat. Maxilloturbinate chamber volume per slice (TC) was used as a surrogate for airway cross-sectional area (all slices within a specimen are of equal thickness so this parameter cancels out) and its value plotted alongside that of TV against slice position from rostral to caudal for canids and felids (Fig. 5). Although maximum maxilloturbinate volume occurs close to its predicted position in both families, the match is not exact. In canids, on average, the airway reaches its greatest cross-sectional area just caudal to maximum turbinate volume, although the two are aligned in three (red fox *Vulpes vulpes*, kit fox, African wild dog) of the eight species. In the seven felids, the opposite occurs. On average, maximum airflow pathway area occurs just before maximum turbinate volume, but the two coincide in the bobcat *Lynx rufus* and African wild cat *Felis sylvestris lybica*.

Maxilloturbinate density within canids

The density of packing of the maxilloturbinates (TV/TC) along the airway varies among species (Fig. 6). As noted above, the typical pattern is for density to increase to a peak and then decline from rostral to caudal. The grey wolf *Canis lupus* exhibits by far the tightest packing of any species, maximally filling nearly 40% of the chamber space (Fig. 6). It is followed by the Brazilian bush dog, which fills at most 31% of its chamber with turbinate bone. The remaining six species are relatively similar, with maximum values ranging from 22% to 26%.

Even though maxilloturbinate density in the African wild dog deviates only moderately from that of the sample average, the architecture of the maxilloturbinates seems to be quite different from that of other species. As can be seen in two representative scans, the African wild dog has a much more open network with an expanded ventral whorl (Fig. 7). By contrast, the wolf has a complex, dendritic

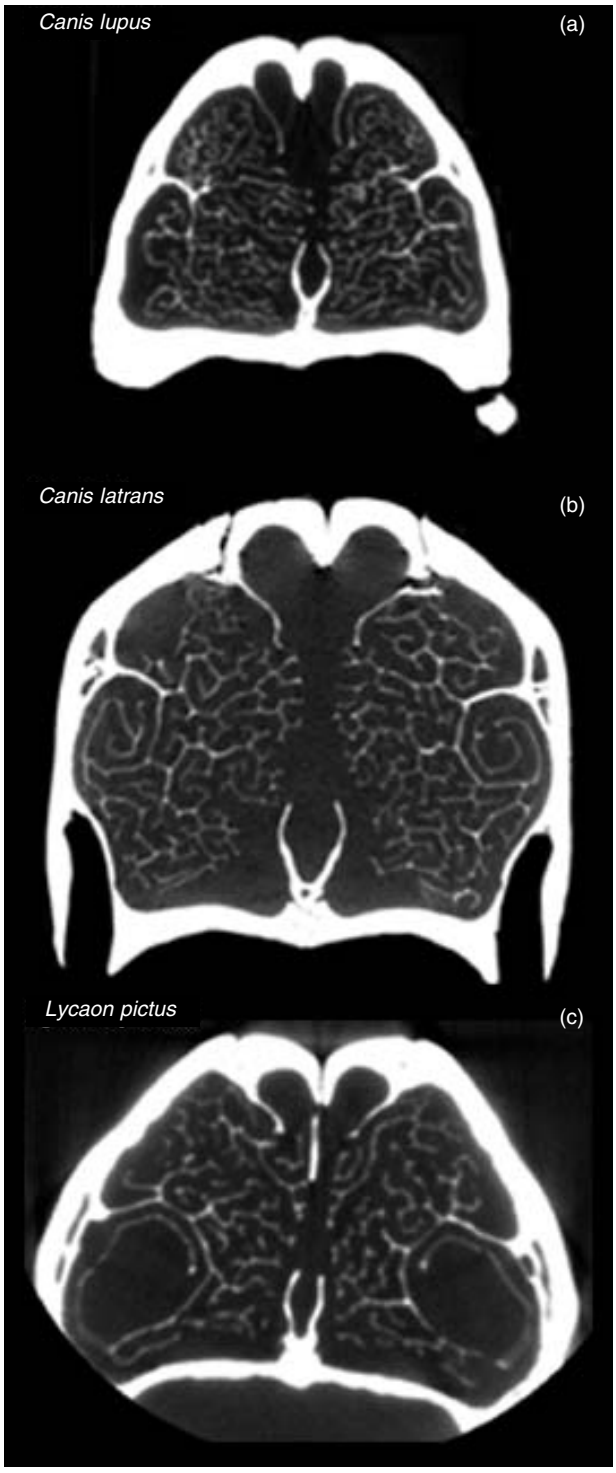

Fig. 7. Coronal CT scans taken at *c.* 50% of length of maxilloturbinates of a grey wolf (a), coyote (b), and African wild dog (c).

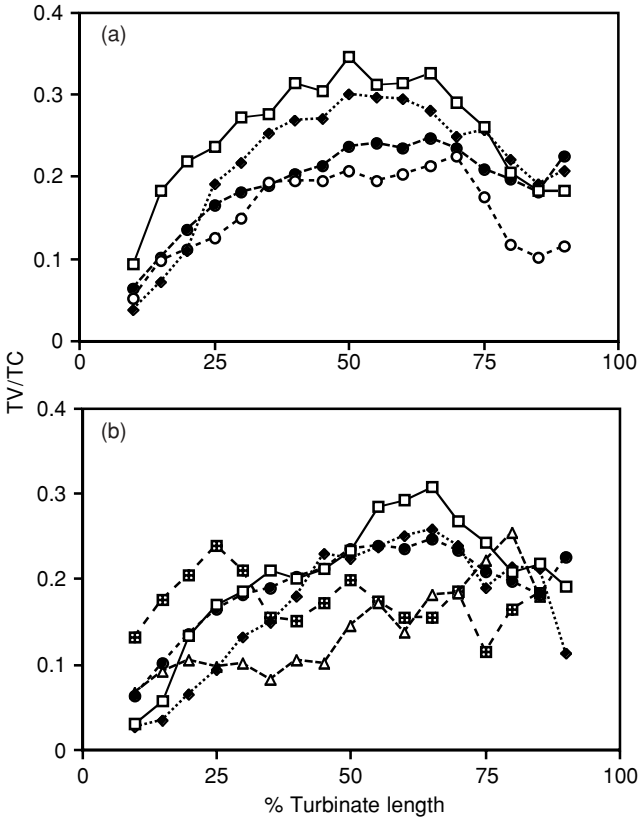

Fig. 8. Average percentage of maxilloturbinate chamber occupied by the maxilloturbinate bones (TV/TC) in 21 coronal slices, taken at 5% intervals from rostral (0) to caudal (100), for each sampled felid. ●, Average of all eight species (both plots). (a) □, Cheetah; ◆, bobcat; ○, African wild cat. (b) □, puma; △, lion; ◆, ocelot; ⊞, leopard.

network with limited expansion of the ventral whorl. The closest relative to the wolf in our sample, the coyote, has maxilloturbinates that are intermediate in density between the wild dog and wolf, and not too different from those of the four fox species.

There is no apparent correspondence between maxilloturbinate packing and body size or habitat. Regressions of TTV/TTC on body mass are not significant ($r^2 = 0.17$, $P = 0.31$). Concerning habitat, the tropical bush dog has more densely packed turbinates than the arctic fox, but they are less dense than those of the temperate to arctic grey wolf. The two arid-living species are not similar; the wild dog has much more loosely packed maxilloturbinates than the kit fox. Even phylogeny explains little of the variation seen in maxilloturbinate packing. The two species of *Canis*, wolf and coyote, differ greatly in turbinate packing, with the coyote displaying a much more open structure. Of the remaining canids, the kit fox and arctic fox are the only other sister taxa (Mercure *et al*., 1993), and are quite similar in the distribution of turbinates from rostral to caudal, with the arctic fox exhibiting a slightly denser network of bone (Fig. 6).

Maxilloturbinate density within felids

The rostral to caudal pattern of maxilloturbinate density varies more among felids than canids (Fig. 8). Whereas the canids (except for the wolf) tended to cluster around an average pattern, the felids are more scattered. Among

the sampled cats, the cheetah displays the densest packing of turbinates but does not quite achieve that seen in the wolf. At the opposite extreme is the lion with relatively open maxilloturbinates, especially rostrally. The leopard is unusual in that maximum maxilloturbinate density occurs in the rostral as opposed to the caudal half of the chamber. Because we were only able to sample a single leopard, this result needs further confirmation with additional specimens.

The marked differences in maxilloturbinate architecture that were apparent among canids (Fig. 7) are also apparent among felids. The densely folded turbinates of the cheetah contrast strongly with the broadly open spirals of the lion (Fig. 9). The probable sister species to the cheetah is the puma *Puma concolor* (Johnson & O'Brien, 1997). Its maxilloturbinates are intermediate in structure; like the cheetah, the turbinates are complexly folded, but like the lion, they are less well developed dorsal to the maxillary stem.

As was true of the canids, the correlation between body size and maxilloturbinate packing (TTV/TTC) is not significant ($r^2 = 0.19$, $P = 0.77$), with the largest (lion) and smallest (ocelot *Leopardus pardalis*) having the least densely packed. Habitat also explains little. The four African species whose ranges and habitats overlap (lion, leopard, cheetah, wild cat) are not more similar to one another than to any other felid in our sample. Similarly, the temperate North American bobcat and puma do not cluster apart from the other felids.

Scaling with body mass

In both canids and felids, total maxilloturbinate volume scales positively with body mass. Felids (slope = 1.47) show a stronger positive allometry than canids (slope = 1.21) and at large size, the two regressions converge (Fig. 10a). Most canids have 1.5–2.0 times the maxilloturbinate volume of felids of similar body mass. Among the canids, the African wild dog and the Arctic fox seem to have relatively the greatest volume of respiratory turbinate for their size. Among the felids, the leopard and cheetah have the largest maxilloturbinates for their size.

Not surprisingly, turbinate chamber dimensions follow the same allometric pattern (Fig. 10b). That is, larger canids and felids have relatively larger turbinate chambers than smaller species, and canids have larger chambers than felids of similar size. However, the leopard and wolf overlap in relative turbinate chamber size. Again, the wild dog and arctic fox fall above the canid regression line, indicating that they have relatively large turbinate chambers.

Unlike the turbinates, nasal chamber volume relative to body mass is similar in both felids and canids (Fig. 10c). It is positively allometric, and seems to be more so in felids than canids, but the slopes do not differ significantly ($P = 0.112$, ANCOVA). The lion has an unusually large snout, but the remaining species cluster close to the regression line ($r^2 = 0.97$).

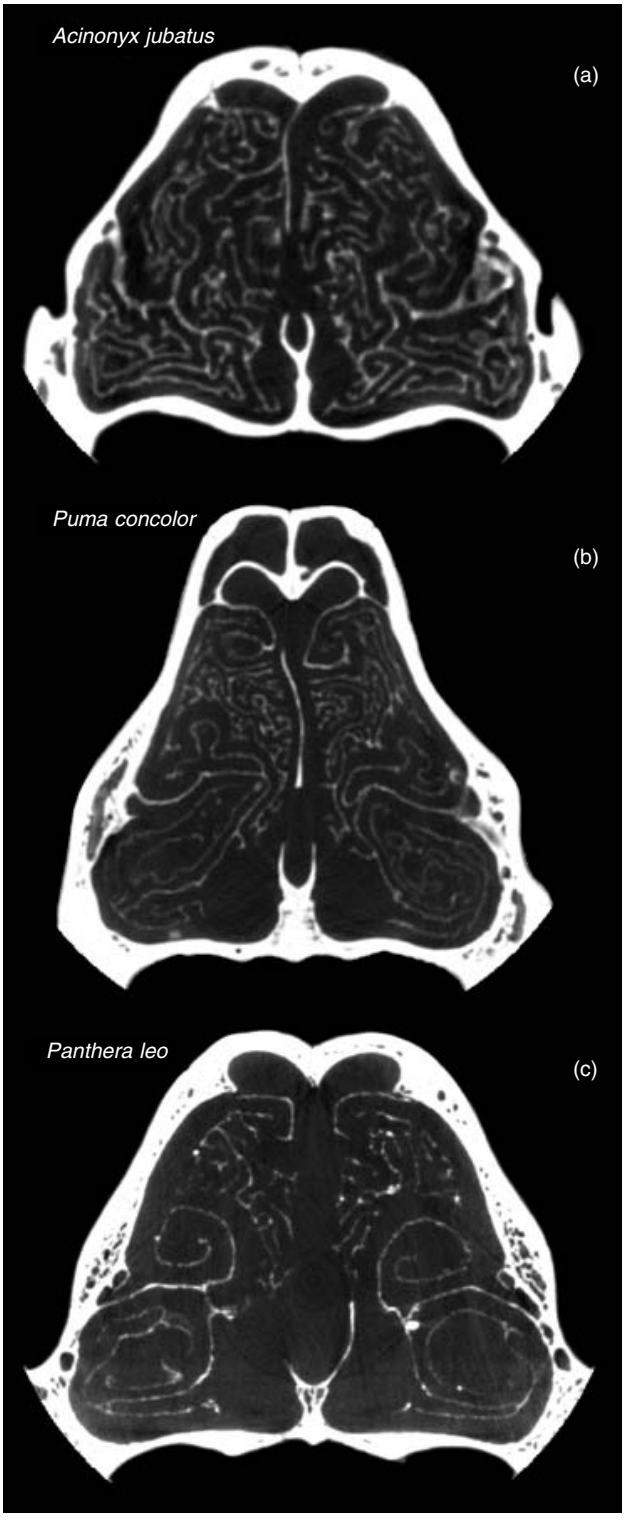

Fig. 9. Coronal CT scans taken at *c.* 50% of length of maxilloturbinates of a cheetah (a), puma (b), and African lion (c).

DISCUSSION

In both canids and felids, total maxilloturbinate chamber volume (TTC) and bone volume (TTV) increased with body size. Thus larger species have relatively more

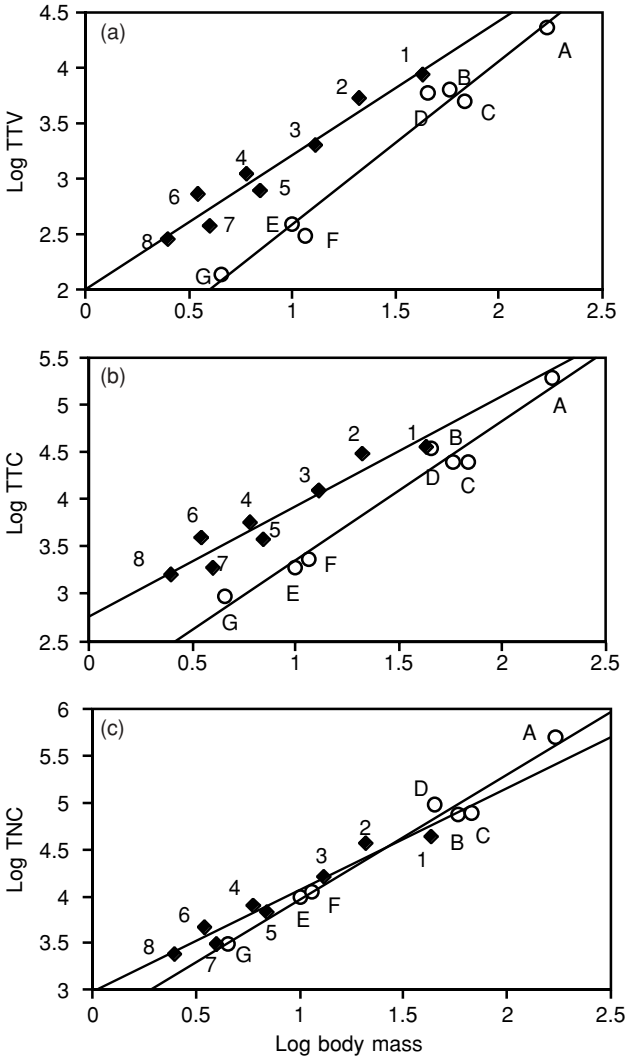

Fig. 10. (a) Linear regression of $\log_{10}$ total maxilloturbinate volume (TTV) against $\log_{10}$ body mass for canids (◆) and felids (○). For canids, $\log_{10}$ TTV = 1.21($\log_{10}$ body mass) + 2.01, $r^2 = 0.94$; for felids $\log_{10}$ TTV = 1.47 ($\log_{10}$ body mass) + 1.12, $r^2 = 0.97$. (b) Linear regression of $\log_{10}$ total maxilloturbinate chamber volume (TTC) against $\log_{10}$ body mass for canids and felids. For canids, $\log_{10}$ TTC = 1.17 ($\log_{10}$ body mass) + 2.76, $r^2 = 0.92$; for felids $\log_{10}$ TTC = 1.47 ($\log_{10}$ body mass) + 1.19, $r^2 = 0.97$. (c) Linear regression of $\log_{10}$ total nasal chamber volume (TNC) against $\log_{10}$ body mass for canids and felids. For canids, $\log_{10}$ TNC = 1.06 ($\log_{10}$ body mass) + 2.89, $r^2 = 0.97$; for felids, $\log_{10}$ TNC = 1.33 ($\log_{10}$ body mass) + 2.63, $r^2 = 0.99$. Species as in Fig. 3.

maxilloturbinate bone and larger chambers than smaller species. This was somewhat surprising because small species are expected to have greater needs for water and heat conservation as a consequence of their reduced surface area relative to volume. Moreover, their snouts are short, reducing the distance over which inhaled air flows and thus the time available for heat and water transfer. Perhaps the size of maxilloturbinates depends more on the volume of air inhaled with each breath, which in turn should follow from lung volume. Lung and trachea volumes scale slightly positively (1.08, lungs; 1.05, trachea) with mass in mammals (Calder, 1984; Schmidt-Nielsen, 1984) but not to the degree observed for maxilloturbinates. Alternatively, it may be that our assumption of similar plate thickness for all species is incorrect. If larger species have thicker maxilloturbinate bones, then bone volume estimates will not be tightly correlated with surface area. Thus the question of the scaling relationship between body mass and the key physiological parameter, surface area, remains unanswered until we can better quantify area.

Relative to body mass, canids have a greater volume (and presumably surface area) of maxilloturbinates than felids. Moreover, the maxilloturbinates of canids are more extensively developed in the dorsal portion of the nasal chamber and have a complex, dendritic appearance. By contrast, the maxilloturbinates of felids are weakly developed dorsally and tend toward a more scroll-like design (Figs 2, 7 & 9). The dorsal expansion of the turbinates seen in canids is replaced in felids by rostral projections of the ethmoturbinates, which are presumed to function in olfaction (Negus, 1958). It is possible that portions of the felid ethmoturbinates and nasoturbinates are covered in respiratory epithelium, as has been observed in some rodents and marsupials (Adams & McFarland, 1972; Kratzing, 1984). If so, then the size of the respiratory turbinate system in felids has been underestimated in our study. Remarkably, despite the extensive use of the domestic cat as a laboratory animal, there is no detailed study of its nasal anatomy. The limited data available suggest that the ethmoturbinates are largely if not entirely olfactory (Negus, 1958; Mills & Christmas, 1990), but this needs to be confirmed by detailed histological work.

Assuming for the moment that felids do have less respiratory turbinates than canids of similar size, it is not what was expected. Because of their relatively short snouts, it was predicted that felids might have a greater volume of maxilloturbinate than canids to compensate for the shorter distance over which inhaled air passes. At a minimum, it was expected that turbinate volume relative to body mass would scale similarly in the two families. The fact that canids seem to have more maxilloturbinates might reflect their greater levels of locomotor activity than felids. In general, canids are more active foragers and more cursorial than felids (Ewer, 1973), and this might be associated with enhanced respiratory abilities, including more extensive maxilloturbinates to minimize water loss with each breath.

Within the maxilloturbinate chamber, the overall density of maxilloturbinate bone is similar in both families. In both, the relationship between total bone volume (TTV) and total chamber volume (TTC) is nearly isometric. This would imply a similar packing of maxilloturbinates within the chamber space in all species and might be expected if there is an optimal gap distance between adjacent bony plates for rapid transfer of heat and water. Schroter & Watkins (1989) found that average gap width varied among the species they studied, ranging from 0.2 mm in the ferret, to 0.4 in cat and dog, to 5 mm in the horse.

In general, larger species had greater average gap widths. Although this might result in less effective heat and water transfer, they argued that this is balanced by the greater distance over which the transfer can occur in larger mammals. According to their model, all the observed gap widths were within a range that would allow ample time for heating and humidification of the air when breathing at rest or under moderate exercise.

In both their study and ours, it was apparent that the volume and density of packing of the maxilloturbinates was not constant over the course of the turbinates in an individual. From rostral to caudal, the volume and the density increase and then decline. Maximum volume and presumed surface area of the maxilloturbinates occurs at or near the point where cross-sectional area of the air pathway is maximal in both canids and felids. This follows expectation because air transit time will be least where the cross-sectional area of the flow is greatest, and this increases the time available for heat and water transfer. Both canids and felids concentrate their maxilloturbinates in the region where most of the transfer is likely to occur.

In both canids and felids, maximum percentage of the maxilloturbinate chamber filled by bone ranged from *c*. 20% to 35% among species (Figs 6 & 8). Among the canids, the species with by far the densest packing of bone within the chamber was the grey wolf. The bush dog also stood out as having relatively densely packed maxilloturbinates along part of their length, but the remaining six canids were fairly similar. The felids varied more interspecifically, with less clustering of species around an average pattern (Fig. 8). The cheetah displays the maximum density of maxilloturbinate packing, with nearly 35% of the chamber filled by bone about halfway along the chamber's length. The largest cat in our sample, the lion, is notable for having a much more loosely packed chamber throughout its length.

These interspecific differences in maxilloturbinate form do not seem to correspond to body size, habitat, or activity pattern. The felid with the densest packing of maxilloturbinates is the cheetah, which might reflect its well-known sprinting ability. Its maxilloturbinate density contrasts sharply with that of the leopard, a sympatric felid of similar size but less cursorial abilities. However, within our sample, the bobcat, a short-distance hunter, comes closest to the cheetah in maxilloturbinate packing.

The variation among the sampled canids was also not easily explained as a result of habitat or body mass differences. The two canids with the densest arrangement of maxilloturbinates are the grey wolf and Brazilian bush dog. One is a large-bodied cursorial hunter in temperate to arctic climates; the other is a small, short-distance rush hunter in tropical rainforest (Bueler, 1973). The ecological parallel (cursorial pack hunter) to the grey wolf is the African wild dog, and its maxilloturbinates are very different in density and architecture (Fig. 7). It is possible that the differences among the species may be better explained by phylogeny than function, but this is difficult to assess based on only eight of 35 canid species. The two most closely related canids in our sample, the kit fox and arctic fox, do differ from one another in the expected direction. That is, the arctic fox, which presumably has greater heat conservation needs than its temperate sister taxon, has slightly denser turbinates and an overall greater volume of turbinate bone for its body size.

The fact that the structure of the maxilloturbinates does not seem to vary dramatically among species that experience distinct heat and water conservation requirements suggests that species may have evolved alternate solutions. That is, it may be simpler, from an evolutionary standpoint, to alter behaviour, pelage, or other characteristics to minimize heat and water loss, rather than change the turbinates. Maxilloturbinates are housed within the skull, a complicated structure that serves multiple critical functions, and changes in any one region are likely to affect other regions. On the other hand, increasing fur density and reducing ear size (e.g. arctic foxes) may be easier solutions to heat conservation needs. Similarly, water conservation can be achieved through behavioural changes, such as resting in burrows (e.g. desert foxes) and foraging during the cooler parts of the day (most species). Notably, in a comparison of desert and non-desert birds, Schmidt-Nielsen *et al*. (1970) were surprised to discover no difference in their ability to restrict respiratory water loss, as estimated by exhaled air temperature. This suggests that desert birds also solve water conservation problems without modifying their respiratory structures.

It seems clear that the relationship of maxilloturbinate form to life habits is not simple. Here, the focus was on the relationship between maxilloturbinate dimensions and the functions of heat and water conservation, but it may be that other constraints are operating as well. For example, the maxilloturbinate chamber serves as a conduit for air moving between the external environment and the lungs. Closely packed maxilloturbinates increase the resistance to airflow (Negus, 1958; Lung & Wang, 1989), perhaps raising the energetic costs of inhalation. Mammals can alter facultatively the size of the gap between highly vascular, adjacent turbinate surfaces by adjusting blood flow. Vasodilation results in increased flow, thickening of the tissue layers lining the turbinates, and consequent decreased gap size. In general, vasodilation occurs as a result of parasympathetic stimulation, and is more likely to occur when the animal is resting. Vasoconstriction diminishes blood flow, increasing gap size, and occurs under sympathetic stimulation (Negus, 1958; Lung & Wang, 1989). In the domestic dog, vasoconstriction results in a 20% drop in airflow resistance (Lung & Wang, 1989). During times of intense exercise, such as when hunting or being pursued, oxygen demand is probably maximal and sympathetic stimulation dominates, producing vasoconstriction and minimal airway resistance, despite the loss of efficiency in heat and water transfer. When resting, vasodilation of the turbinate tissues will decrease gap width and enhance the efficiency of water and heat conservation, including selective brain cooling. Indeed, recent studies of free-ranging African ungulates (Jessen *et al*., 1994; Mitchell, Maloney, Laburn *et al*., 1997; Maloney *et al*., 2002) indicate that selective brain cooling usually occurs during late afternoon rest when parasympathetic

stimulation is likely to be prevalent. However, it is not known as yet whether carnivorans behave similarly.

Our high-resolution scans of maxilloturbinates reveal a greater structural complexity than was apparent from previous studies based on dissections. In some species, such as the African wild dog, there are clear differences in gap distance between plates in a single coronal section. Along much of the length of their turbinates, African wild dogs display a greatly expanded ventral whorl combined with a more typical dendritic dorsal extension (Fig. 7). Is the ventral whorl a low resistance air pathway that functions primarily during long distance pursuits of prey? Because of coupling between respiration and locomotion, galloping tetrapods are limited to a single breath with each stride (Bramble & Carrier, 1983). The skulls of wild dogs are expanded laterally relative to the other canids sampled, enlarging the width of the air pathway. African wild dogs are champions among canids in their ability to run extremely fast for long distances (Estes & Goddard, 1967; Creel & Creel, 2002), and it is tempting to think that the broad nasal chamber and open architecture of their maxilloturbinates relate to their aerobic capacity. It is probable that the density of blood vessels varies over the surface of the turbinates, and vasodilation/vasoconstriction could allow complex adjustments of airflow under differing demands for oxygen supply, heat and water conservation.

This study has opened a number of new avenues for research on respiratory turbinates. It further demonstrated that CT technology could resolve the extremely fine structure of the bony turbinates, opening the door for more studies of additional species. Our initial analyses of maxilloturbinate volume relative to body size suggest tight scaling within the two families, with felids tending to show greater positive allometry than canids, but this should be tested with a larger sample of species. Previous work that suggested that maximum turbinate volume occurs where cross-sectional area of the chamber is greatest is confirmed. We are currently working on developing new approaches to estimating surface area as well as average gap width. More data on the distribution of vasculature across the turbinates, as well as olfactory and respiratory epithelium would be extremely useful. Using the CT scans, a three-dimensional model of the maxilloturbinates can be constructed which might then be used to understand better the flow patterns within these intricate structures. Because respiratory turbinates were probably a critical element in the evolution of mammalian endothermy (Hillenius, 1992), a better understanding of their function(s) should provide insights into the therapsid to mammal transition.

Acknowledgements

For access to computers, we thank Dr A. Toga of the UCLA Brain Imaging Center and Drs P. Hoffmann and P. Lechner of the UCLA Visualization lab. We are especially grateful to C. Holmes for assistance with the program MNI Display. We thank R. Ketcham and the staff of the University of Texas High Resolution CT scanning laboratory for scanning the specimens and advice on data analysis, and curators at the Field Museum of Natural History (Chicago), Natural History Museum of Los Angeles County, and the Museum of Vertebrate Zoology (UC Berkeley) for allowing us to borrow and scan their specimens. P. Adam, W. J. Hillenius, R. Hunt, J. Sedlmayr, S. J. Vogel, R. K. Wayne and N. Wideman provided helpful comments on the paper.

REFERENCES

Adams, D. R. & McFarland, L. Z. (1972). Morphology of the nasal fossae and associated structures of the hamster (*Mesocricetus auratus*). *J. Morphol*. **137**: 161–180.

Baker, M. A. (1982). Brain cooling in endotherms in heat and exercise. *Annu. Rev. Physiol*. **44**: 85–96.

Bramble, D. M. & Carrier, D. R. (1983). Running and breathing in mammals. *Science* **219**: 251–256.

Bueler, L. E. (1973). *Wild dogs of the world*. NewYork: Stein and Day.

Calder, W. A. III. (1984). *Size, function and life history*. Boston: Harvard University Press.

Collins, J. C., Pilkington, T. C. & Schmidt-Nielsen, K. (1971). A model of respiratory heat transfer in a small mammal. *Biophys. J*. **11**: 886–914.

Creel, S. & Creel, N. M. (2002). *The African wild dog: behavior, ecology, and conservation*. Princeton, NJ: Princeton University Press.

Estes, R. D. & Goddard, J. (1967). Prey selection and hunting behavior of the African wild dog. *J. Wildl. Manage*. **31**: 52–70.

Evans, H. E. (1993). *Miller's anatomy of the dog*. 3rd edn. Philadelphia, PA: W. B. Saunders.

Ewer, R. F. (1973). *The carnivores*. Ithaca, NY: Cornell University Press.

Goldberg, M. B., Langman, V. A. & Taylor, C. R. (1981). Panting in dogs: paths of air flow in response to heat and exercise. *Respir. Physiol*. **43**: 327–338.

Hayward, J. N. & Baker, M. A. (1969). A comparative study of the role of the cerebral arterial blood in the regulation of brain temperature in five mammals. *Brain Res*. **16**: 417–440.

Hillenius, W. J. (1992). The evolution of nasal turbinates and mammalian endothermy. *Paleobiology* **18**: 17–29.

Huntley, A. C., Costa, D. P. & Rubin, R. D. (1984). The contribution of nasal counter-current heat exchange to water balance in the Northern elephant seal, *Mirounga angustirostris*. *J. exp. Biol*. **113**: 447–454.

Jessen, C., Laburn, H. P., Knight, M. H., Kuhnen, G., Goelst, K. & Mitchell, D. (1994). Blood and brain temperatures in free-ranging black wildebeest in their natural environment. *Am. J. Physiol*. **36**: R1528–R1536.

Jessen, C. (2001). *Temperature regulation in humans and other mammals*. Berlin: Springer-Verlag.

Joeckel, R. M., Peigne, S., Hunt, R. M. & Skolnick, R. L. (2002). The auditory region and nasal cavity of Oligocene Nimravidae (Mammalia: Carnivora). *J. Vertebr. Paleontol*. **22**: 830–847.

Johnson, W. E. & O'Brien, S. J. (1997). Phylogenetic reconstruction of the Felidae using 16s rRNA and NADH-5 mitochondrial genes. *J. Mol. Evol*. **44**(Suppl.): S98–S116.

Kratzing, J. E. (1984). The anatomy and histology of the nasal cavity of the koala (*Phascolarctos cinereus*). *J. Anat*. **138**: 55–65.

Langman, V. A., Maloney, G. M. O., Schmidt-Nielsen, K. & Schroter, R. C. (1979). Nasal heat exchange in the giraffe and other large mammals. *Respir. Physiol*. **37**: 325–332.

Lung, M. A. & Wang, J. C. (1989). Autonomic nervous control of nasal vasculature and airflow resistance in the anesthetized dog. *J. Physiol*. **419**: 121–129.

Mahoney, S. K., Fuller, A., Mitchell, G. & Mitchell, D. (2002). Brain and arterial blood temperatures of free-ranging oryx (*Oryx gazella*). *Eur. J. Physiol*. **443**: 437–445.

Mercure, A., Ralls, K., Koepfli, K. P. & Wayne, R. K. (1993). Genetic subdivisions among small canids: mitochondrial DNA differentiation of swift, kit, and arctic foxes. *Evolution* **47**: 1313–1328.

Mills, R. P. & Christmas, H. E. (1990). Applied comparative anatomy of the nasal turbinates. *Clin. Otolaryngol*. **15**: 553–558.

Mitchell, D., Maloney, S. K., Laburn, H. P., Knight, M. H., Kuhnen, G. & Jessen, C. (1997). Activity, blood temperature and brain temperature of free-ranging springbok. *J. Comp. Physiol. B biochem. syst. environ. Physiol*. **167**: 335–343.

Mitchell, D., Maloney, S. K., Jessen, C., Laburn, H. P., Kamerman, P. R., Mitchell, G. & Fuller, A. (2002). Adaptive heterothermy and selective brain-cooling in arid-zone mammals. *Comp. Biochem. Physiol. B comp. Physiol*. **131**: 571–585.

Negus, V. (1958). *The comparative anatomy and physiology of the nose and paranasal sinuses*. Edinburgh: E. & S. Livingstone.

Schmidt-Nielsen, K. (1984). *Scaling: why is animal size so important*? Cambridge: Cambridge University Press.

Schmidt-Nielsen, K., Hainworth, F. R. & Murrish, D. F. (1970). Counter-current exchange in the respiratory passages: effect on water and heat balance. *Respir. Physiol*. **9**: 263–276.

Schroter, R. C. & Watkins, N. V. (1989). Respiratory heat exchange in mammals. *Respir. Physiol*. **78**: 357–368.

Sunquist, M. & Sunquist, F. (2002). *Wild cats of the world*. Chicago: University of Chicago Press.

Van Valkenburgh, B. (1987). Skeletal indicators of locomotor behavior in living and extinct carnivores. *J. Vertebr. Paleontol*. **7**: 162–182.

Van Valkenburgh, B. & Koepfli, K. P. (1993). Cranial and dental adaptations for predation in canids. In *Mammals as predators: Symposia of the Zoological Society of London* No. 65: 15–37. Dunstone, N. & Gorman, M. L. (Eds). Oxford: Oxford University Press.

Vogel, S. (2003). *Comparative biomechanics: life's physical world*. Princeton, NJ; Princeton University Press.